Applied Geochemistry 102 (2019) 129–138

Contents lists available at ScienceDirect

Applied Geochemistry

journal homepage: www.elsevier.com/locate/apgeochem

Long-term sorption and desorption of uranium in saprolite subsoil with nanoporous goethite

Hun Bok Jung[a,*], Huifang Xu[b], Eric E. Roden[b]

[a] Department of Earth and Environmental Sciences, New Jersey City University, Jersey City, NJ, United States
[b] Department of Geoscience, University of Wisconsin, Madison, WI, United States

ARTICLE INFO

Keywords:
Uranium
Saprolite
Sorption
Desorption
Nanoporous goethite

ABSTRACT

Long-term (2–3 months) batch U(VI) sorption-desorption experiments were conducted to understand the long-term sorption-desorption behavior of U(VI) in saprolite subsoils from Oak Ridge Field Research Center (ORFRC), Tennessee, which contained naturally occurring nanoporous goethite. Three subsoil samples containing a range of dithionite-citrate-bicarbonate (DCB) extractable Fe oxide content (7138, 11,161, and 22,582 mg Fe/kg) were used for the experiments. Sorption of 50 μM U(VI) to the subsoils in the presence of Ca^{2+} and HCO_3^- at circumneutral pH occurred rapidly during the first 2 days, after which slow U(VI) sorption continued over 3 months. U(VI) desorption from the soils by 10 mM $NaHCO_3$ solution exhibited an initial fast desorption step during the first 24 h, followed by slower desorption over a week. Sorption of 50 μM U(VI) for 1 day to 3 months in the presence or absence of Ca^{2+} consistently resulted in higher U(VI) sorption to saprolite soil with higher amount of nanoporous goethite, while desorption of U(VI) for 1 week to 2 months was consistently lower in saprolite soil with higher amount of nanoporous goethite. Saprolite subsoils containing higher amounts of nanoporous goethite exhibited more resistant U(VI) desorption, and the proportions of irreversible U(VI) sorption increased with longer residence time with soils. These results indicates that more U(VI) became bound to the internal surfaces of nanoporous iron oxides during long-term sorption. This study suggests that naturally occurring nanoporous goethite may exert a significant role in controlling the mobility and transport of U(VI) in historically contaminated sites that have existed over decades.

1. Introduction

While uranium (U) is a naturally occurring radioactive element in the earth's crust (average 3 ppm), anthropogenic activities such as the mining and milling of uranium ores, generation of nuclear energy, and storage of legacy waste have contaminated water, sediment, and soil in many parts of the world (Baborowski and Bozau, 2006; Maher et al., 2013; Campbell et al., 2015). In the US, there are a number of uranium contaminated sites of U.S. Department of Energy (DOE), including the Savannah River, Oak Ridge, and Hanford sites where a variety of radionuclides are present (Fox et al., 2012). The major health effect of uranium is chemical kidney toxicity, rather than a radiation hazard (Kurttio et al., 2002).

Sorption and desorption of contaminants to/from natural soils and sediments is of central importance to most environmental concerns because sorption-desorption affects geochemical fate, toxicity, and associated risk to human and aquatic life as well as the efficiency of most remediation technologies (Kan et al., 1998). The mobility, toxicity, and bioavailability of uranium in natural environments are controlled by uranium speciation, oxidation-reduction, and sorption-desorption processes. Oxidized hexavalent uranium, U(VI) is highly soluble, whereas the solubility of U(IV) is largely controlled by insoluble oxides such as uraninite (UO_2) (Maher et al., 2013). Aqueous speciation of U(VI) is affected by pH, bicarbonate, and Ca^{2+} concentrations. At moderate bicarbonate concentrations above neutral pH, U(VI) speciation is dominated by uranyl-carbonato complexes [e.g., UO_2CO_3(aq), $UO_2(CO_3)_2^{2-}$, $UO_2(CO_3)_3^{4-}$] in the absence of Ca^{2+}, while calcium-uranyl-carbonato ternary complexes [e.g., $Ca_2UO_2(CO_3)_3^0$ (aq), $CaUO_2(CO_3)_3^{2-}$] are dominant in the presence of Ca^{2+} in typical groundwater (Guillaumont et al., 2003; Dong and Brooks, 2006; Fox et al., 2006). The primary aqueous species of uranium in groundwater of many uranium contaminated sites such as the Old Rifle site and the Oak Ridge Field Research Center are known to be calcium-uranyl-carbonato ternary species (Anderson et al., 2003; Yabusaki et al., 2007; Kelly

* Corresponding author. Department of Earth and Environmental Sciences, New Jersey City University, 2039 Kennedy Boulevard, Jersey City, NJ, 07305, United States.

E-mail address: hjung@njcu.edu (H.B. Jung).

https://doi.org/10.1016/j.apgeochem.2019.01.017
Received 28 July 2018; Received in revised form 12 November 2018; Accepted 31 January 2019
Available online 01 February 2019
0883-2927/ © 2019 Elsevier Ltd. All rights reserved.

et al., 2008).

A great number of studies have investigated the mobility and transport of U(VI) in synthetic Fe or Al oxides, as well as natural sediments and soils by short term batch and column experiments on a time scale typically less than a week (Hsi and Langmuir, 1985; Waite et al., 1994; Barnett et al., 2000, 2002; Sylwester et al., 2000; Davis et al., 2004; Fox et al., 2006; Stewart et al., 2010; Dong et al., 2012; Dong and Wan, 2014). However, there is little information on the long-term (months-years) partitioning of U(VI) at the soil-water interface, while a few previous studies conducted long term sorption-desorption experiments with goethite (6 months sorption) and mesoporous silica (2 weeks sorption and 2 weeks desorption) (Giammar and Hering, 2001; Singer et al., 2014). Because there is a growing body of evidence that sorption and desorption may not reach equilibrium within time scales of short term experiments, batch sorption experiments may require significantly longer reaction to reach equilibrium (Ball and Roberts, 1991). The bioavailability of metals has been reported to decrease with an increased residence time due to ageing processes, resulting in irreversible reactions (Ainsworth et al., 1994; Ford et al., 1997; Eick et al., 1999; Trivedi and Axe, 2000; Arai and Sparks, 2002). Different sorption and desorption behaviors of metals or radionuclides between short term and long term experiments (Bruemmer et al., 1988; Eick et al., 1999; Ahmed et al., 2008) may result in inconsistent prediction of contaminant transport in the subsurface. Because contamination and remediation in the natural environment usually occur over many years, it is important to understand long-term equilibrium and rate of sorption-desorption of contaminants. Current knowledge is insufficient to understand the long term irreversibility of U(VI) sorption, although the reversibility of sorption controls the geochemical mobility and bioavailability of U(VI) in the contaminated soils and sediments.

This study investigated long term U(VI) sorption-desorption reactions at the saprolite soil-water interface by batch experiments on a time scale of 2–3 months. Natural saprolite subsoils from Oak Ridge Field Research Center (ORFRC) contain various amounts of nanoporous goethite, which has shown to play a significant role in regulating U(VI) sorption-desorption behavior on a time scale of days to weeks (Jung et al., 2016). Natural ferric iron oxides (e.g., ferrihydrite, goethite, and hematite), which are widely thought to be the most important sorbents for U(VI) under circumneutral pH (Hsi and Langmuir, 1985; Waite et al., 1994; Bargar et al., 1999; Giammar and Hering, 2001; Wazne et al., 2003; Fox et al., 2006), are likely nanoporous in sediments/soils due to the aggregation of nanoparticles (Banfield et al., 2000; van der Zee et al., 2003; Gilbert et al., 2009). Nanoporous minerals have been reported to provide the most reactive surface area for geochemical reactions (Wang et al., 2003, 2010; Hochella, 2008; McBriarty et al., 2017).

In order to better predict the mobility and transport of U(VI) in contaminated subsurface environments and to improve the efficiency of environmental remediation, it is necessary to have a thorough understanding of the mechanisms of uranium sorption and desorption over extended periods of time. The objectives of this study are to understand the effects of residence time on the sorption and desorption of U(VI) in saprolite soil from the Oak Ridge Field Research Center (ORFRC), Tennessee and to evaluate the role of natural nanoporous goethite in controlling the long term U(VI) sorption-desorption processes.

2. Materials and methods

2.1. Sample preparation and characterization

Subsurface saprolite soil cores were collected from the Area 2 site of the Oak Ridge Field Research Center (ORFRC), which was established within the Y-12 National Security Complex area on the Department of Energy's Oak Ridge Reservation in Oak Ridge, TN (Moon et al., 2006). The core sections collected at 6.5–9 m depth below the ground surface were air-dried, sieved through a 2 mm sieve, and then thoroughly homogenized. A portion of sample was extracted with 10% nitric acid (1.6 N; Fisher, trace metal grade) for 2 days to determine the concentration of acid-extractable solid phase uranium, while the amount of Fe oxides (e.g., goethite, ferrihydrite) was determined by the dithionite-citrate-bicarbonate (DCB) extraction (Jackson, 1986). Based on DCB extractable Fe, three soil samples (~80% sand and ~20% silt and clay) containing a range of Fe oxide content (7138, 11,161, and 22,582 mg/kg Fe) and background levels of U (< 0.01 μmol/g by 10% HNO_3 for 2 days) were selected, which are referred to as low Fe soil, medium Fe soil, and high Fe soil, respectively in this study. Specific surface area and pore size distribution were determined by BET (Brunauer-Emmett-Teller) method and BJH (Barrett-Joyner-Halenda) method, respectively using a surface area and pore size analyzer (NOVA e4200, Quantachrome Instruments) (Jung et al., 2016). The standard reference material (Quantachrome Instruments; 108 m^2/g) confirmed that the analytical error was less than ± 5%.

Minerals in three saprolite soil samples were identified by X-ray diffraction analyses using a Rigaku Rapid II X-ray diffraction system with a 2-D image plate (Mo Kα radiation), while high resolution images of goethite nano-crystals were provided by TEM (Transmission Electron Microscope) and SAED (Selected Area Electron Diffraction) measurements using a FEI Titan 80–200 FEG-TEM/STEM microscope equipped with an X-ray EDS (Energy Dispersive Spectroscopy) analyzer and Gatan Image Filtering (GIF) system (Jung et al., 2016).

2.2. Batch sorption-desorption experiments

One gram of dry soil was placed in a 15 mL plastic centrifuge tube (Fisher Scientific), and 10 mL of a 0.1 M $NaNO_3$ solution containing 50 μM U(VI)-acetate, 2–5 mM $NaHCO_3$, and 0–2.5 mM $Ca(NO_3)_2$ was added. Dissolved Ca^{2+} and HCO_3^- are common ions in groundwater and have a significant impact on the aqueous speciation of U(VI) as well as the sorption and mobility of U(VI) in aquifers because of the formation of uranyl calcium carbonate and uranyl carbonato species (Fox et al., 2006). The solution pH was initially adjusted to ~6.5 by adding 0.1 N HNO_3 or 0.1 N NaOH. The initial pH and final pH were measured using a pH meter (Accumet XL20, Fisher Scientific). Sorption experiments were conducted mostly in duplicates.

The tubes were shaken at 250 rpm for 2 days to 3 months for the U(VI) sorption kinetics experiments in the presence of 50 μM U(VI), 2.5 mM Ca^{2+} and 5 mM HCO_3^-. After the reaction for 2 days, 7 days, 14 days, 1 month, 2 months, and 3 months, the supernatant was collected by centrifugation at 3000 rpm for 10 min and was analyzed for U(VI). Afterwards the remaining soil samples were subjected to desorption in 10 mL of a 10 mM $NaHCO_3$ solution for 1 week. Another sets of U(VI) sorption experiments were conducted in a 0.1 M $NaNO_3$ solutions containing 50 μM U(VI) and 2 mM HCO_3^- for 1 week and in a 0.1 M $NaNO_3$ solutions containing 50 μM U(VI), 2.5 mM Ca^{2+} and 5 mM HCO_3^- for 3 months. After the sorption experiments, the soil samples were exposed to a 10 mM $NaHCO_3$ solution for 2 weeks and 2 months. Additional sorption experiments were conducted in a 0.1 M $NaNO_3$ solution containing 50 μM U(VI), 2.5 mM Ca^{2+}, and 5 mM HCO_3^- for 1 day and 1 month. Subsequently, sequential desorption of U(VI) was performed in 10 mL of 10, 100, and 1000 mM $NaHCO_3$ solutions for 3 weeks (1 week for each desorption step). $NaHCO_3$ solutions were used for desorption of U(VI) from soils because the bicarbonate extraction has been shown to effectively release reversible, adsorbed U from contaminated sediments (Kohler et al., 2004).

After sorption and desorption experiments, dissolved U(VI) concentrations were determined using a kinetic phosphorescence analyzer (KPA-11) (ChemChek Instruments, Richland, WA) (Brina and Miller, 1992). Analytical error was less than ± 5%. Sorbed U(VI) was determined by the difference between the initial and final aqueous U(VI) concentrations.

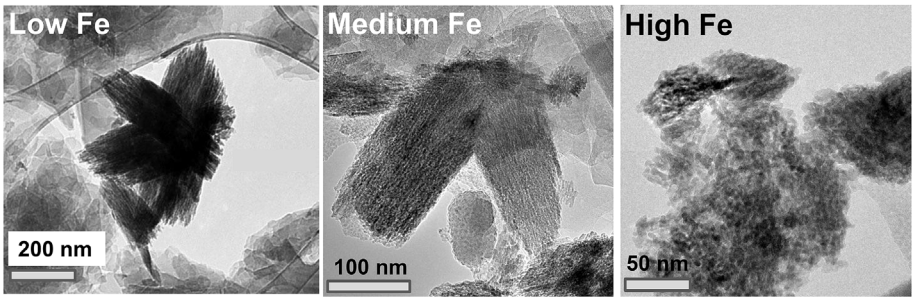

Fig. 1. High-resolution transmission electron microscopy (TEM) images of nano-goethite in saprolite subsoils from the Oak Ridge Field Research Center (ORFRC). Goethite nano-crystals are more crystalline in the low Fe soil than in the medium Fe soil or the high Fe soil, while goethite in the high Fe soil was dominated by aggregates of poorly crystalline nano-crystals whose structure state was between ideal goethite and ferrihydrite.

3. Results

3.1. Characteristics of the ORFRC saprolite subsoils

The characterization of saprolite subsoils from ORFRC using XRD, TEM, as well as BET and BJH methods has previously been reported in Jung et al. (2016). Major minerals identified by XRD were quartz, illite and smectite, while nano-goethite was observed in all three soil samples by TEM (Fig. 1). Nano-goethite was closely associated with illilte/smectite (I/S), and exhibited nanocrystalline and nanoporous structures, particularly in the medium and high Fe soils (Fig. 1). Goethite in the high Fe soil was dominated by aggregates of poorly crystalline nano-crystals with an average size of ~5 nm. The structural state of goethite nano-crystals in the high and medium Fe soils was between ideal goethite and ferrihydrite. Therefore the amount of Fe oxides determined by the DCB extraction represented both goethite and ferrihydrite. Goethite may be formed through oriented aggregation of its precursor ferrihydrite nano-crystals. High-resolution TEM images exhibited nanopore spaces between goethite nano-crystals (Fig. 1). Goethite nano-crystals were less abundant and more crystalline in the low Fe soil than in the medium Fe soil or the high Fe soil, resulting in less nanoporous surfaces.

TEM-EDS analysis showed that U(VI) sorption in those saprolite soils was associated mainly with nanoporous goethite aggregates rather than clay minerals (Jung et al., 2016). BET specific surface area was 25, 29, and 38 m^2/g for the low, medium, and high Fe soil samples, respectively. Nanoporosity determined by BJH method for the low, medium, and high Fe soil samples was 1.5, 2.0, and 1.9 μL/g for pore size < 2 nm, and 16.3, 18.4, and 30.4 μL/g for pore size < 10 nm, respectively (Jung et al., 2016). BJH pore volume for larger pores with size between 10 nm and 120 nm was 19.1, 20.1, and 56.4 μL/g for the low, medium and high Fe soil samples, respectively (Barrett et al., 1951).

3.2. Speciation of aqueous U(VI) during sorption

The pH of aqueous solution was initially adjusted to 6.5 and increased to 7.1–7.2 in 1 month and then to 7.3–7.4 in 3 months during sorption reaction with three soil samples. Nonetheless, it is unlikely that the change of pH significantly affected the sorption of U(VI) given that the maximum sorption of U(VI) by iron oxides occurs at circumneutral pH between 6 and 8 (Hsi and Langmuir, 1985; Waite et al., 1994; Wazne et al., 2003). PHREEQC modeling (Parkhurst and Appelo, 1999) was performed to predict the speciation of U(VI) at equilibrium pH of 6.5–7.5 using the databases from Bernhard et al. (2001) and Guillaumont et al. (2003), while the LLNL.dat database (a database file in PHREEQC) was used to calculate saturation indices for U phases (Bernhard et al., 2001; Guillaumont et al., 2003). At equilibrium pH of 6.5–7.5, uranyl-calcium-carbonato ternary species (e.g., $Ca_2UO_2(CO_3)_3$, $CaUO_2(CO_3)_3^{2-}$) account for 81–87% of total U(VI) in the presence of 2.5 mM Ca^{2+} and 5 mM HCO_3^-, while uranyl-carbonato species (e.g., $UO_2(CO_3)_2^{2-}$, $UO_2(CO_3)_3^{4-}$, UO_2CO_3) account for 13–19% of total U (VI). In the presence of 2 mM HCO_3^- without Ca^{2+}, uranyl-carbonato species represent nearly all U(VI) species at pH 6.5–7.5. All solutions for sorption experiments were undersaturated with respect to U-bearing phases such as schoepite [$(UO_2)_8O_2(OH)_{12}\cdot 12(H_2O)$] and rutherfordine ($UO_2CO_3$).

3.3. Sorption kinetics of U(VI) over 3 months

U(VI) sorption kinetics experiments were conducted in the presence of 2.5 mM Ca^{2+} and 5 mM HCO_3^- over 3 months. Initial sorption of U (VI) for 2 days occurred rapidly and then slower U(VI) sorption continued to occur over 3 months (Fig. 2). In the first 2 days, 16%, 27%, and 50% of added 50 μM U(VI) were sorbed to the low Fe, medium Fe, and high Fe soil samples, respectively. Over the period of 3 months, the percentage of U(VI) sorption increased to 57%, 67%, and 94% for the low, medium and high Fe soil samples, respectively (Fig. 2). This corresponded to sorption of 0.28, 0.33, and 0.47 μM U(VI)/g (Fig. 2A) and distribution coefficient (Kd) of 13, 20, and 149 mL/g (Fig. 2B) for the low, medium and high Fe soil samples, respectively. U(VI) sorption was higher for soil samples with higher Fe content, which is consistent with

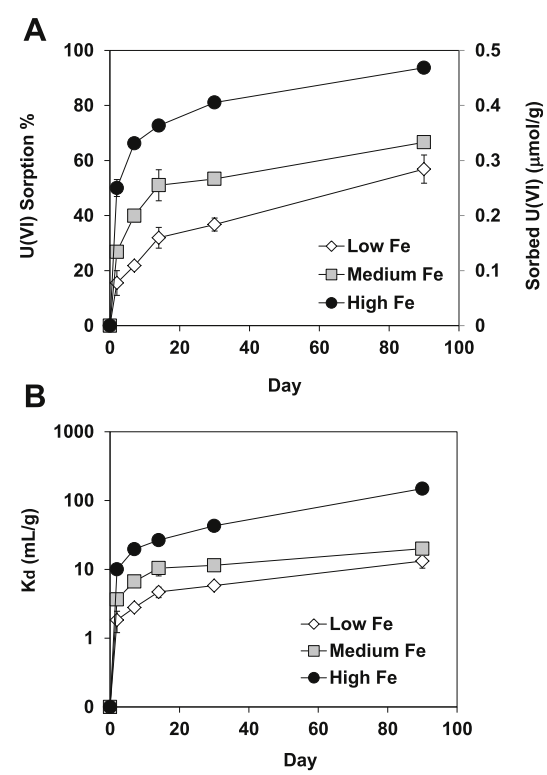

Fig. 2. Sorption kinetics (**A**: sorption % and amount of sorbed U(VI); **B**: distribution coefficient, Kd) of 50 μM U(VI) to 1 g of the ORFRC soils in 10 mL of 0.1 M $NaNO_3$ solution containing 2.5 mM Ca^{2+} and 5 mM HCO_3^- at pH of ~7 over 3 months. The plotted data show the average of duplicate samples with error bars representing standard deviation.

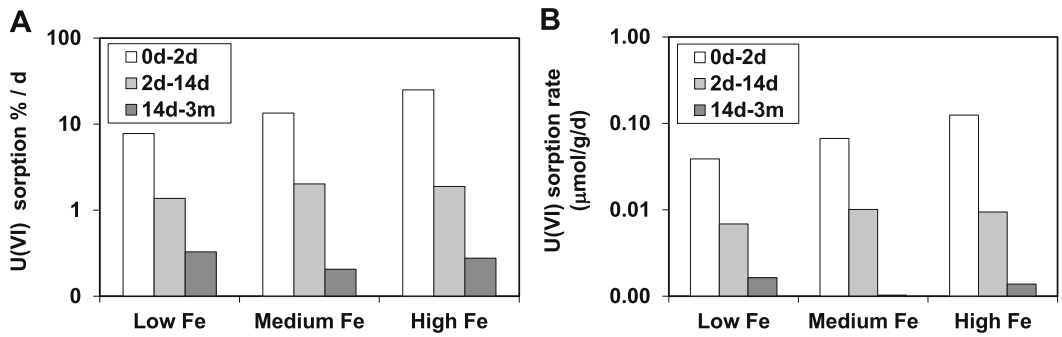

Fig. 3. Change of U(VI) sorption rate (**A**: sorption%/day and **B**: μmol/g/day) during sorption over a period of 3 months (day 0 to day 2, day 2 to day 14, and day 14 to day 90) for the low Fe, medium Fe, and high Fe soils.

the previous results from short term U(VI) sorption experiments over 2 days to 2 weeks (Jung et al., 2016).

The rates of U(VI) sorption changed over 3 months, exhibiting 3 distinct stages. U(VI) sorption rate was highest in the first 2 days for all three soil samples, in which the U(VI) sorption rate was 8% sorption per day for the low Fe soil, 13% sorption per day for the medium Fe soil and 25% sorption per day for the high Fe soil (Fig. 3A). This corresponded to the sorption rate of 0.039–0.125 μmol U(VI)/g per day (Fig. 3B). Then U(VI) sorption rate decreased remarkably between 2 days and 2 weeks, ranging from 1.4% sorption per day to 2.0% sorption per day, which were equivalent to U(VI) sorption of 0.007–0.010 μmol/g per day (Fig. 3). U(VI) sorption rate further decreased to 0.2–0.3% sorption per day between 2 weeks and 3 months, which corresponded to U(VI) sorption of 0.001–0.002 μmol/g per day (Fig. 3). The U(VI) sorption rate was significantly higher in soil samples with higher Fe content during the first 2 days, whereas it was similar for all soil samples during the sorption period between 2 days and 3 months.

3.4. Desorption kinetics of U(VI) over 1 week

After U(VI) sorption to soil samples for 2 days, 1 week, 1 month, or 3 months, the soil samples were subjected to desorption experiments by 10 mM $NaHCO_3$ solution for a week to remove U(VI) bound to reversible sorption sites. Kohler et al. (2004) showed that the bicarbonate extraction method using the 20 mequiv/L sodium bicarbonate/carbonate solution was useful for estimating the mass of reversible U(VI) in sediments. For all soil samples, U(VI) desorption occurred rapidly in the first 24 h, and then continued slowly over a week (Fig. 4). For the low Fe soil, U(VI) desorption percentage [desorbed U(VI)/sorbed U (VI) × 100] during the first 24 h was 30–42%, and then increased continuously to 38–76% during a week of desorption (Fig. 4A). As a result, sorbed U(VI) decreased from 0.08-0.30 μmol/g to 0.02–0.18 μmol/g (Fig. 4D). For the medium Fe soil, the extent of U(VI) desorption after 24 h ranged from 31% to 45%, while it increased to 41–59% after 1 week (Fig. 4B). Consequently, U(VI) sorbed to the medium Fe soil samples decreased from 0.18-0.33 μmol/g to 0.07–0.20 μmol/g (Fig. 4E). For the high Fe soil, U(VI) desorption percentage was 23–48%, and then increased to 37–63% after 1 week (Fig. 4C). Accordingly, sorbed U(VI) decreased from 0.25-0.47 μmol/g to 0.14–0.33 μmol/g after 1-week desorption (Fig. 4F).

The results showed that a longer period of U(VI) sorption generally led to lower extent of U(VI) desorption and higher amount of U(VI) remaining in soils (Fig. 4). The percentage of U(VI) desorption for a week was significantly lower for the medium Fe soil (43–59%) and high Fe soil (37–63%) than for the low Fe soil (57–76%) after U(VI) was sorbed to soils for 2 days to 1 month, while U(VI) desorption percentage was similar for all soils after sorption of U(VI) for 3 months, ranging from 38% to 41%. The U(VI) desorption kinetics results were characterized with a rapid initial desorption (0–1 day) followed by slower desorption that continued between day 1 and day 7 (Fig. 5). For the 2-day sorption to 3-month sorption samples, U(VI) desorption rates were 30–42% per day for the low Fe soil, 31–45% per day for the medium Fe soil, and 23–48% per day for the high Fe soil during the first day, while it decreased to 1–6%, 1–2%, and 1–3% per day for the low, medium, and high Fe soils, respectively during the desorption from day 1 to day 7 (Fig. 5).

3.5. Long term desorption of U(VI) over 2 weeks and 2 months

Prior to long term U(VI) desorption, U(VI) sorption experiments were conducted with a 0.1 M $NaNO_3$ solution containing 50 μM U(VI) and 2 mM HCO_3^- for 1 week and with a 0.1 M $NaNO_3$ solution containing 50 μM U(VI), 2.5 mM Ca^{2+} and 5 mM HCO_3^- for 3 months. Uranyl calcium carbonate species were dominant with 2.5 mM Ca^{2+} and 5 mM HCO_3^-, while uranyl carbonato species were the predominant species with 2 mM HCO_3^-. Regardless of the speciation of uranium, U(VI) sorption was consistently higher in the soil with higher Fe content (Fig. 6). For the 1-week sorption in the presence of HCO_3^-, sorption percentage ranged from 41% to 96%, which corresponded to the amount of sorbed U(VI) from 0.20 to 0.48 μmol/g (Fig. 6A) and distribution coefficient (Kd) of 7–227 mL/g for the low to high Fe soils (Fig. 6B). For the 3-month sorption in the presence of Ca^{2+} and HCO_3^-, sorption percentage was 66–89% (Fig. 6A). This corresponded to the concentrations of sorbed U(VI) from 0.33 to 0.45 μmol/g and Kd of 20–86 mL/g for the low to high Fe soils (Fig. 6A and B). For the medium and high Fe soils, the 3-month sorption percentage (75 and 89%) was lower than the 1-week sorption percentage (82 and 96%) despite the longer period of sorption, which is attributed to the formation of uranyl calcium carbonate species in the presence of Ca^{2+} and HCO_3^- for the 3-month sorption experiments. It has been reported that uranyl calcium carbonate complexes adsorb weakly to iron oxides and sediments (Fox et al., 2006; Stewart et al., 2010). Uranyl calcium carbonate species may dominates U(VI) aqueous speciation in many uranium-contaminated aquifers containing both Ca^{2+} and HCO_3^- as major cations and anions. In contrast, for the low Fe soil, sorption percentage was still higher when sorption occurred for 3 months (66%) than for 1 week (41%) despite the presence of uranyl calcium carbonate species (Fig. 6).

After the U(VI) sorption experiments for 1 week in the presence of HCO_3^-, the soil samples were subsequently reacted with 10 mM $NaHCO_3$ solution over 2 weeks and 2 months to desorb reversibly bound U(VI). The 2-week desorption and 2-month desorption results were similar for all soil samples (Fig. 7A and B). For the low Fe soil, U (VI) desorption percentage was 58% and 67% for the 2-week and 2-month desorption, respectively. For the medium Fe soil, U(VI) desorption percentage was 49% and 43% for the 2-week and 2-month desorption, respectively, while for the high Fe soil, U(VI) desorption percentage was 45% and 41% for the 2-week and 2-month desorption, respectively. This resulted in U(VI) of 0.09, 0.21, and 0.26 μmol/g remaining in the low, medium, and high Fe soil samples, respectively after 2 weeks of desorption, while U(VI) remaining in the low, medium

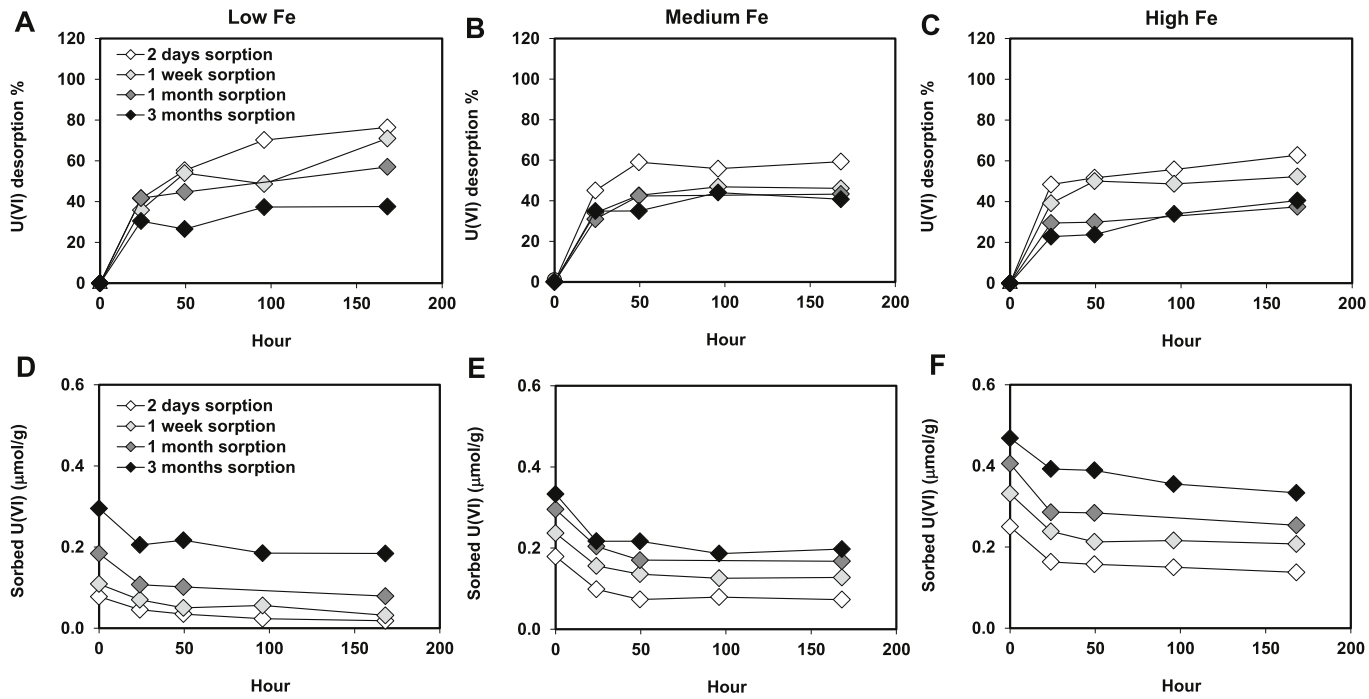

Fig. 4. Percentage of U(VI) desorption and the amount of U(VI) sorbed to saprolite soils (A and D: low Fe, B and E: medium Fe and C and F: high Fe) during the 1-week desorption by 10 mM $NaHCO_3$ solution after sorption of 50 μM U(VI) in the presence of 2.5 mM Ca^{2+} and 5 mM HCO_3^- over 2 days, 1 week, 1 month, and 3 months.

and high Fe soils was 0.07, 0.23, and 0.28 μmol/g, respectively after desorption for 2 months (Fig. 7B).

After the 3-month U(VI) sorption in the presence of Ca^{2+} and HCO_3^-, U(VI) desorption by 10 mM $NaHCO_3$ solution over 2 weeks and 2 months occurred to a similar extent for the medium and high Fe soils (Fig. 7C). The percentage of U(VI) desorption over 2 weeks and 2 months was 45% and 55%, respectively for the medium Fe soil, while it was 33% and 36%, respectively for the high Fe soil. In contrast, the 2-month U(VI) desorption was significantly higher than the 2-week U(VI) desorption for the low Fe soil. While the U(VI) desorption percentage was 55% after 2 weeks, it increased to 92% after 2 months (Fig. 7C). As a result, U(VI) remaining in the low, medium, and high Fe soil samples was 0.15, 0.21, and 0.30 μmol/g, respectively after 2 weeks of desorption, whereas it was 0.03, 0.17, and 0.29 μmol/g, respectively after 2 months of desorption (Fig. 7D).

3.6. Sequential desorption of U(VI) over 3 weeks

Sorption experiments were conducted in a 0.1 M $NaNO_3$ solution containing 50 μM U(VI), 2.5 mM Ca^{2+}, and 5 mM HCO_3^- for 1 day and 1 month (Fig. 8). After 1 day of sorption, sorption percentage was 15%, 34%, and 54% for the low, medium, and high Fe soils, which was equivalent to U(VI) sorption of 0.07, 0.17, and 0.27 μmol/g (Fig. 8). U (VI) sorption percentage increased to 34%, 58%, and 80% after 1 month of sorption for the low, medium, and high Fe soils, respectively, which were equivalent to U(VI) sorption of 0.17, 0.29, and 0.40 μmol/g. Accordingly, distribution coefficients (Kd) for the low, medium, and high Fe soils were 2, 5, and 12 mL/g, respectively for the 1-day sorption, while they were 5, 14, and 41 mL/g for the 1-month sorption (Fig. 8).

After the U(VI) sorption, U(VI) was extracted from the soil samples sequentially by 10 mM $NaHCO_3$ solution for 1 week, by 100 mM $NaHCO_3$ solution for 1 week, and then by 1000 mM $NaHCO_3$ solution for 1 week. For the 1-day sorption samples, the U(VI) desorption percentage increased to 73% and 72% for the low and medium Fe soils, respectively during the 1-week desorption by 10 mM $NaHCO_3$ solution (Fig. 9A and B), while the U(VI) desorption percentage increased to 47% for the high Fe soil over a week (Fig. 9C). For the 1-month sorption samples, the percentage of U(VI) desorption by 10 mM $NaHCO_3$ solution increased to 64% for the low Fe soil, to 46% for the medium Fe soil, and to 34% for the high Fe soil over a week (Fig. 9A–C).

Subsequent extraction of the 1-day sorption samples by 100 mM $NaHCO_3$ solution showed that U(VI) desorption percentage increased from 73 to 88% for the low Fe soil, from 72% to 90% for the medium Fe soil, and from 47% to 72% for the high Fe soil over a week (Fig. 9A–C). For the 1-month sorption samples, U(VI) desorption percentage for the low, medium, and high Fe soils increased from 64% to 84%, from 46% to 67%, and from 34% to 69%, respectively over a week. Finally, additional U(VI) desorption by 1000 mM $NaHCO_3$ solution for a week resulted in nearly complete U(VI) desorption by ~90–100% for all samples (Fig. 9A–C). This suggests that 1000 mM $NaHCO_3$ solution is capable of extracting U(VI) from virtually all sorption sites of nano-goethite in the soils.

The U(VI) remaining in soils gradually decreased during the sequential desorption (Fig. 9D–F). For the 1-day sorption samples, the concentrations of U(VI) in the low, medium and high Fe soils decreased from 0.07-0.27 μmol/g to 0.02–0.14 μmol/g by the 10 mM HCO_3 extraction, to 0.01–0.07 μmol/g by the 100 mM HCO_3 extraction, and then to ≤ 0.01 μmol/g by the 1000 mM HCO_3 extraction, respectively. For the 1-month sorption samples, the concentrations of U(VI) in the low, medium and high Fe soils decreased from 0.17-0.40 μmol/g to 0.06–0.26 μmol/g by the 10 mM HCO_3 extraction, to 0.03–0.12 μmol/g by the 100 mM HCO_3 extraction, and then to 0.01–0.04 μmol/g by the 1000 mM HCO_3 extraction, respectively.

Although the extent of U(VI) desorption from the low Fe soil by the 10 mM HCO_3 extraction was comparable between the 1-day sorption and 1-month sorption samples, U(VI) desorption from the medium Fe and high Fe soils by the 10 mM HCO_3 extraction was significantly lower for the 1-month sorption samples than the 1-day sorption samples (Fig. 9A–C). In addition, the percentage of U(VI) desorption by the 10 mM and 100 mM HCO_3 extractions was lower for the medium and high Fe soils than for the low Fe soil, which was more evident for the 1-

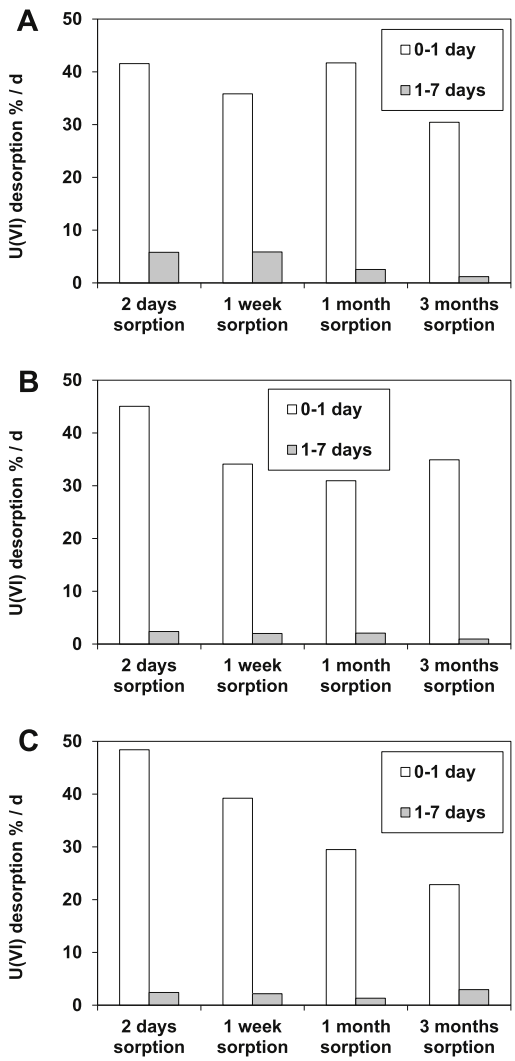

Fig. 5. U(VI) desorption rate in % per day (first 1 day and day 1 to day 7) during the 1-week desorption by 10 mM $NaHCO_3$ solution after sorption of 50 μM U(VI) to the low Fe soil (A), the medium Fe soil (B), and the high Fe soil (C) over 2 days, 1 week, 1 month, and 3 months in the presence of 2.5 mM Ca^{2+} and 5 mM HCO_3^-.

month sorption samples than the 1-day sorption samples.

4. Discussion

4.1. Long term multi-step U(VI) sorption-desorption kinetics

Although U(VI) sorption is known to occur rapidly (Giammar and Hering, 2001; Fox et al., 2006), the long term U(VI) sorption results showed that U(VI) sorption did not reach equilibrium in several days or weeks and continued to occur over 3 months in all soils with low to high Fe content (Fig. 2). There were three distinct stages of U(VI) sorption kinetics: 0–2 days, 2 days-2 weeks, and 2 weeks-3 months (Fig. 3). The initially rapid sorption of U(VI) within a few hours to days followed by a slower sorption of U(VI) over weeks to months can be attributed to rapid sorption of U(VI) to external surfaces of goethite and slow diffusion of U(VI) into internal nanopores of goethite (Bruemmer et al., 1988). U(VI) desorption also occurred in multiple steps: rapid desorption of U(VI) within 24 h and slow desorption of U(VI) over a week (Fig. 4). The two-step U(VI) desorption behavior is attributed to the initial fast desorption of U(VI) bound to external surfaces of goethite

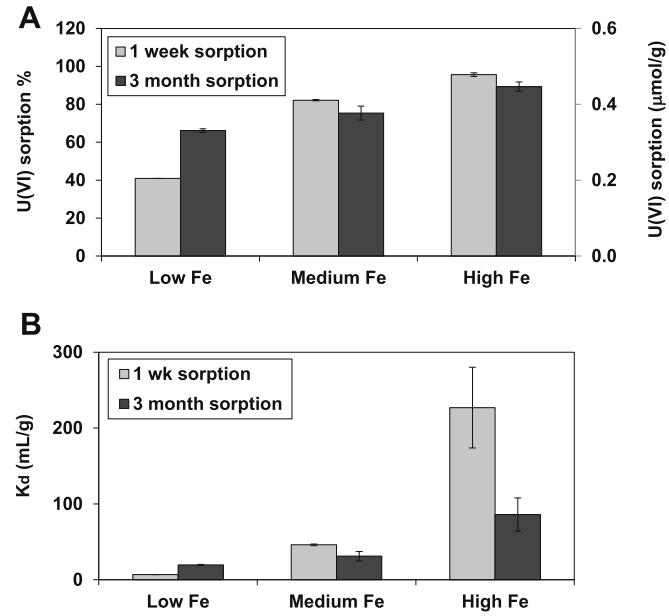

Fig. 6. Sorption of 50 μM U(VI) (**A**: U(VI) sorption % and amount of sorbed U (VI); **B**: distribution coefficient, Kd) to saprolite soils in 0.1 M $NaNO_3$ solution for 1 week (with 0 mM Ca^{2+} and 2 mM HCO_3^-) and 3 months (with 2.5 mM Ca^{2+} and 5 mM HCO_3^-). The plotted data are the average of duplicate samples with error bars representing standard deviation.

and the subsequent slower desorption of U(VI) from internal nanoporous surfaces of goethite (Wang et al., 2003; Jung et al., 2016).

While the U(VI) sorption and desorption reactions in sediments have been frequently treated as equilibrium reactions (Barnett et al., 2002; Davis et al., 2004; Curtis et al., 2006; Loganathan et al., 2009), recent studies found that U(VI) surface complexation is a kinetic process (Qafoku et al., 2005; Liu et al., 2008, 2009; Fox et al., 2012; Stoliker et al., 2013), rate-limited by mass transfer in intragranular and intergranular domains in sediments (Bai et al., 2009; Liu et al., 2009; Stubbs et al., 2009). The initial rapid sorption reaction is generally considered as a reversible sorption step, while the second, slower sorption reaction has been described as a partly irreversible sorption process (Li et al., 2012).

The experimental results from this study showed that the slow U(VI) sorption process during the period of 2 days–3 months was more dominant than the rapid U(VI) sorption during the first 2 days for the low and medium Fe soils (Fig. 2). The U(VI) sorption that occurred in the low, medium, and high Fe soils during the first 2 days accounts for 27%, 40%, and 53% of total U(VI) sorption over 3 months, respectively, while the U(VI) sorption that occurred between 2 days and 3 months represented 73%, 60%, and 47% of total U(VI) sorption, respectively (Fig. 2A). The amount of U(VI) sorbed to the low, medium and high Fe soils was 0.08, 0.13, and 0.25 μmol/g, respectively during the first 2 days, while it was similar for all soil samples during the sorption period between day 2 and day 90, ranging from 0.20 to 0.22 μmol/g (Fig. 2A). The significant extent of U(VI) sorption to all soil samples with low to high Fe content after the first 2 days suggests that there were sufficient nanoporous surfaces (pore size $<$ 10 nm) to slowly bind U(VI) not only in the medium Fe and high Fe soils (18.4 and 30.4 μL/g) but also in the low Fe soil (16.3 μL/g) (Jung et al., 2016).

4.2. Irreversible sorption of U(VI) to nanoporous goethite

In this study, U(VI) desorption by 10 mM $NaHCO_3$ solution for a week was not complete for all soil samples with sorption period ranging from 2 days to 3 months (Fig. 4). The percentage of U(VI) desorption was 38–76% for the low Fe soil samples, 41–59% for the medium Fe soil

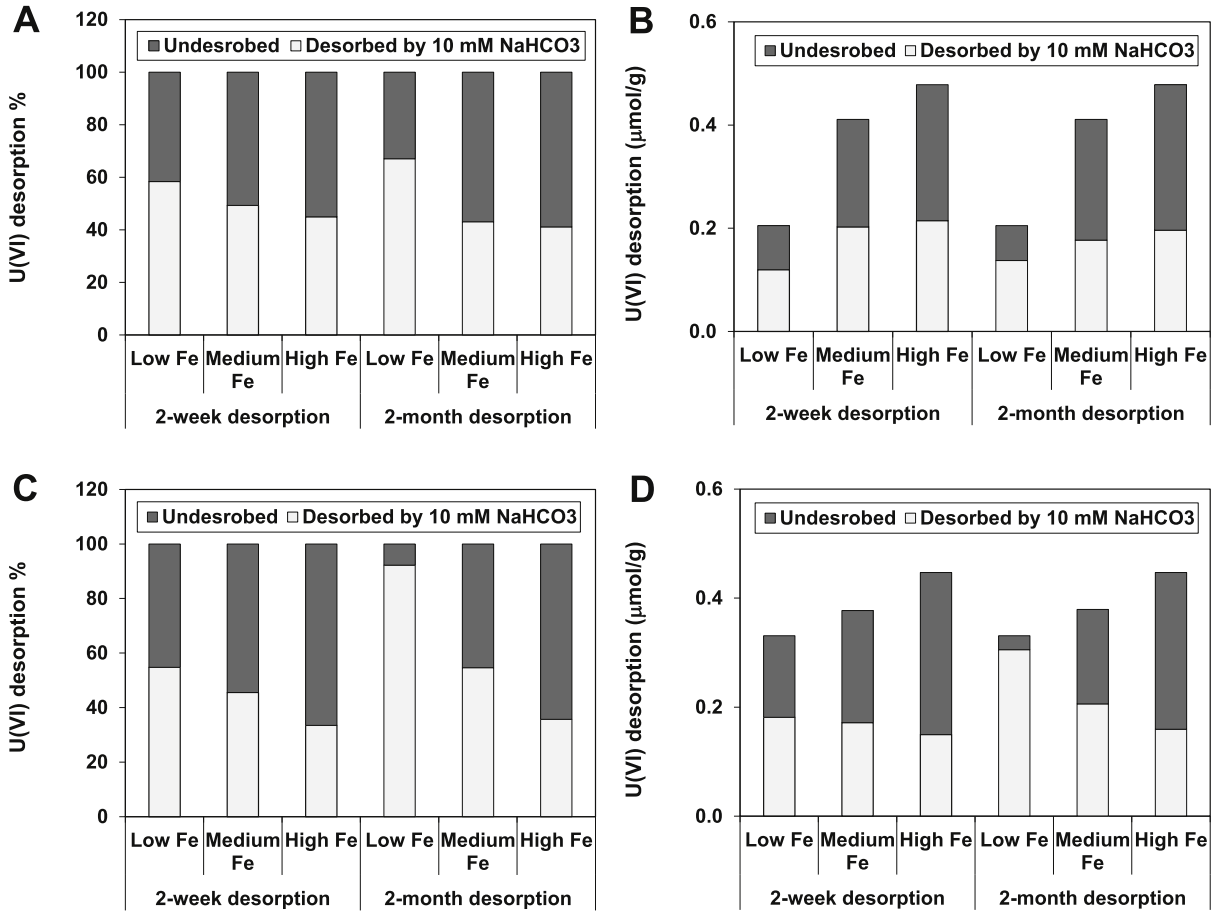

Fig. 7. Desorption of U(VI) from saprolite soils by 10 mM $NaHCO_3$ solution over 2 weeks and 2 months after sorption of 50 μM U(VI) in the presence of 2 mM HCO_3^- for 1 week (A and B) and in the presence of 2.5 mM Ca^{2+} and 5 mM HCO_3^- for 3 months (C and D).

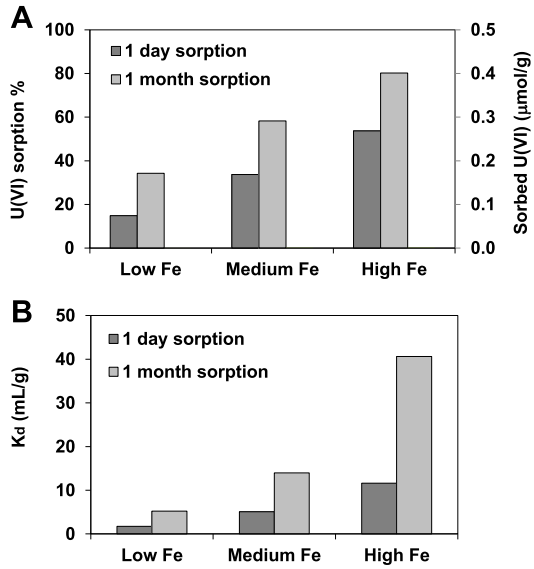

Fig. 8. Sorption of 50 μM U(VI) to saprolite soils in 0.1 M $NaNO_3$ solutions containing 2.5 mM Ca^{2+} and 5 mM HCO_3^- for 1 day and 1 month (**A**: U(VI) sorption % and amount of sorbed U(VI); **B**: distribution coefficient, Kd).

samples, and 37–63% for the high Fe soils. The U(VI) that is resistant to the 10 mM $NaHCO_3$ extraction over a week can be considered irreversible in a typical shallow groundwater aquifer. Kohler et al. (2004) estimated the labile fraction of U(VI) in U-contaminated aquifer sediments obtained from a former U mill tailings site at Naturita, CO by the sodium bicarbonate/carbonate (14.4 mM $NaHCO_3$ and 2.8 mM Na_2CO_3) extraction. Accordingly, irreversible U(VI) ranged from 0.02 to 0.33 μmol/g, which increased with higher Fe content. This indicates that significant amounts of U(VI) were bound irreversibly to the saprolite soils. It has been reported that 10–100 mM HCO_3 extraction removed U(VI) only partially from U(VI) contaminated sediments or soils (Phillips et al., 1995; Gadelle et al., 2001; Curtis et al., 2004; Kohler et al., 2004). Numerous previous studies also have shown that sorption-desorption reactions of heavy metals are often not completely reversible (McLaren et al., 1986, 1998; Ainsworth et al., 1994; Backes et al., 1995). The irreversible sorption behavior has been attributed to solid-state diffusion within oxide particles (Bruemmer et al., 1988), diffusion into micropores and intraparticle spaces (Ball and Roberts, 1991; Backes et al., 1995), change in the type of surface complex (McBride, 1994), and incorporation into the mineral structure via recrystallization (Ainsworth et al., 1994).

Based on the 10 mM $NaHCO_3$ extraction results, the irreversibility of U(VI) generally increased with higher content of nanoporous goethite (Figs. 4, 7 and 9), which suggests that nanoporous goethite was most likely responsible for irreversible sorption of U(VI) in the saprolite soils. Nanopores may greatly affect the sorption-desorption behavior of U(VI) because of their high internal surface area and nanopore confinement effects (Senapati and Chandra, 2001; Wang et al., 2003; Jung et al., 2012; Wang, 2014). A strong time-dependence of sorption and non-reversible desorption behavior that are frequently observed in natural soil or sediment, have been attributed to the effect of nanopores or micropores (Pignatello and Xing, 1996; Jeon et al., 2004; van Beinum et al., 2005; Hochella, 2008). Internal pore domains within subsurface

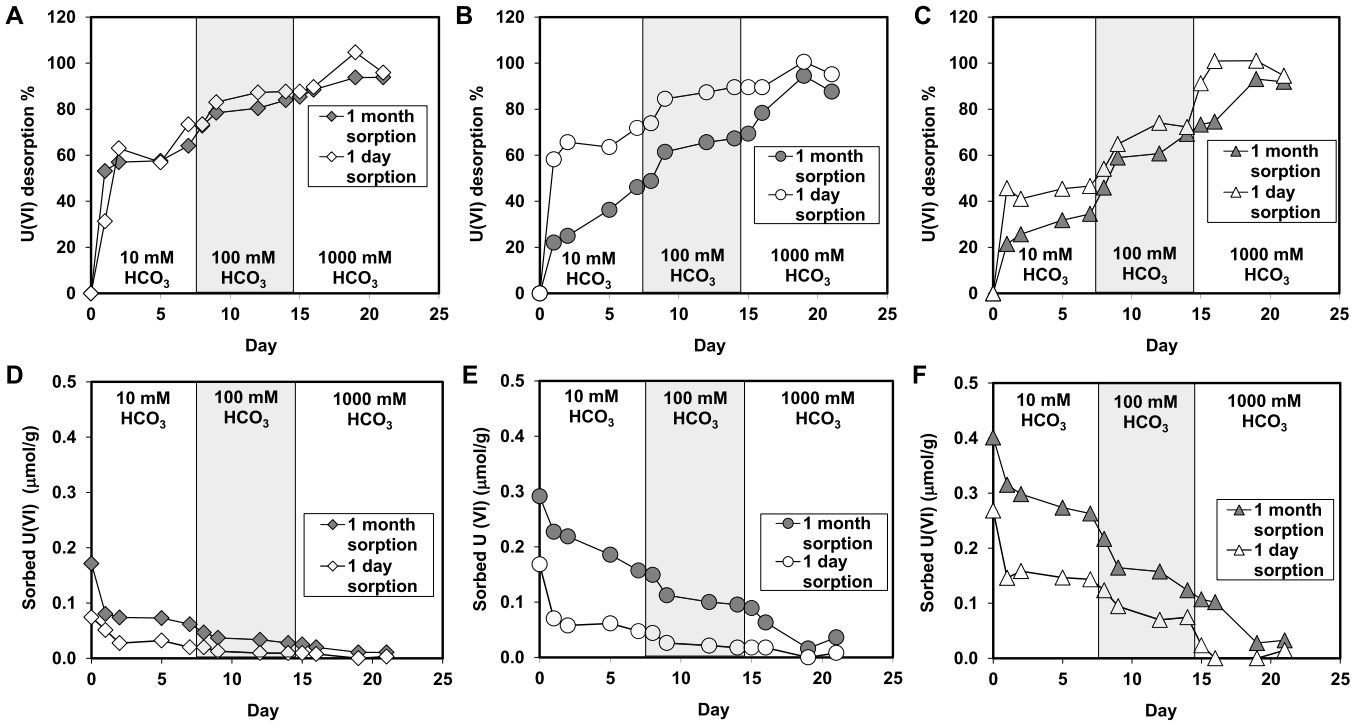

Fig. 9. Sequential desorption kinetics of U(VI) by 10, 100, and 1000 mM $NaHCO_3$ solutions for a total of 3 weeks (1 week for each desorption step) after sorption of 50 μM U(VI) to saprolite soils (Low Fe: A and D, Medium Fe: B and E, High Fe: C and F) in 0.1 M $NaNO_3$ solutions containing 2.5 mM Ca^{2+} and 5 mM HCO_3^- for 1 day and 1 month.

sediments and soil contain a significant fraction of their porosity as nanopores, which may dominate the reactive surface area of diverse media types (Zachara et al., 2016). It has been hypothesized that surface chemical processes such as adsorption-desorption in pores ranging between 1 and 100 nm should be different from larger ones because of (1) confinement-induced changes in water properties and their effects on solvation and electrical double layer, and (2) surface curvature effects on site density, surface charge, and counterion condensation (Abbas et al., 2008; Prelot et al., 2011; Ferreira et al., 2012). As the pore width reduces to 5 nm or less, the interfacial regions of opposing surfaces begin to overlap, reducing the diffusivity of aqueous species in the pore center to values below bulk, while, for pore widths smaller than 2 nm, layered water structures overlap strongly and diffusivity becomes highly sensitive to pore size (Zachara et al., 2016).

4.3. Effects of residence time on U(VI) desorption

The amount of sorbed U(VI) that was resistant to desorption by 10 mM HCO_3^- increased with increasing prior time of sorption and with increasing Fe content (Fig. 10). More U(VI) became irreversibly associated with sorption sites with increasing prior sorption time perhaps because U(VI) initially bound to external sorption sites moved to internal sorption sites within nanoporous goethite as the residence time increased (Backes et al., 1995). This highlights the important role of nanoporous minerals, which provide internal sorption surfaces, in controlling the mobility and bioavailability of U(VI) in aged soils or sediments of historically contaminated sites. When U(VI) was sorbed over 1 day to 1 month, the percentage of U(VI) that was resistant to the 10 mM HCO_3 extraction was significantly higher in the soil samples with higher content of nano-goethite (Fig. 10A and B), which suggests that more internal sorption sites are present in the medium and high Fe soils than in the low Fe soil. In contrast, the percentage of irreversibly bound U(VI) was similar for all soil samples, ranging approximately from 60% to 70% when U(VI) sorption occurred for 3 months

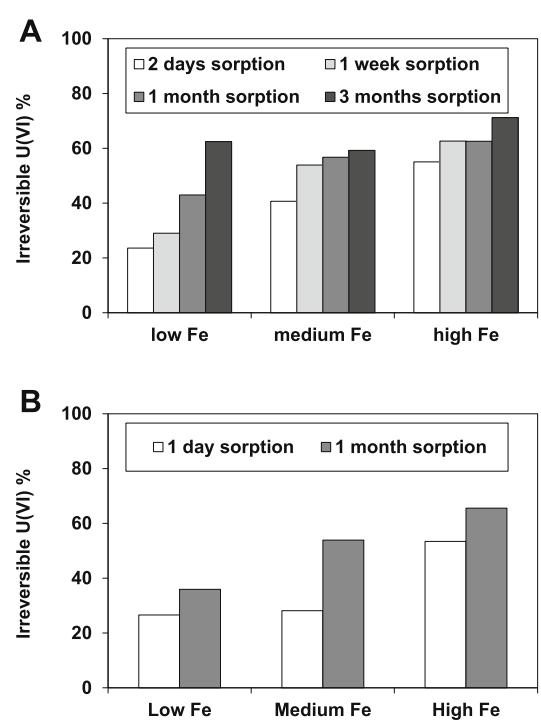

Fig. 10. Percentage of U(VI) that is resistant to desorption by 10 mM $NaHCO_3$ solution after sorption of 50 μM U(VI) to saprolite soils (Low Fe, Medium Fe, and High Fe) in the presence of 2.5 mM Ca^{2+} and 5 mM HCO_3^- for 2 days to 3 months (A) and for 1 day and 1 month (B).

(Fig. 10A). It is also notable that the increase in the percentage of irreversibly bound U(VI) with increasing period of sorption was more evident for the low Fe soil than for the medium Fe soil or high Fe soil

(Fig. 10). This suggests that it took more time for U(VI) to be irreversibly bound to soils containing lower nano-goethite content. However, with sufficient contact time, a significant quantity of U(VI) can become resistant to desorption even in soils or sediments containing low amount of nanoporous minerals, which is referred to as a residence time/aging effect (Pignatello and Xing, 1996). Residence time effects by soils and soil minerals have been previously documented for organic contaminants and trace elements (Steinberg et al., 1987; Ainsworth et al., 1994; Backes et al., 1995; Hatzinger and Alexander, 1995; McLaren et al., 1998; Eick et al., 1999). Numerous explanations have been given to explain the observed residence time effect, including the formation of multinuclear surface complexes or surface precipitates, solid-state diffusion, micropore diffusion, and a change in the surface complex (Eick et al., 2001). Further study is needed to better understand mechanisms of the residence time effect on U(VI) sorption to naturally occurring nanoporous goethite in aged contaminated soils.

4.4. Conclusions and environmental implications

The U(VI) sorption to the ORFRC saprolite soils containing nanoporous goethite in the presence of 0–2.5 mM Ca^{2+} and 2–5 mM HCO_3^- at circumneutral pH, occurred rapidly during the first 2 days and then slowly increased over 3 months. U(VI) desorption from the soils by 10 mM $NaHCO_3$ solution exhibited an initial fast desorption step during the first 24 h, followed by a slow desorption step over 1 week. More irreversible U(VI) desorption occurred in the soil with higher amount of nanoporous goethite. Desorption of U(VI) by 10–100 mM $NaHCO_3$ solutions resulted in partial and incomplete desorption of U(VI) from the saprolite soils. Desorption-resistant fraction of U(VI) increased with increasing sorption period, which indicates that aging led to a reduction of reversible U(VI) fraction perhaps due to the increasing sorption of U (VI) to irreversible sites within nanopores of goethite with longer residence time.

The effects of residence time on the sorption-desorption of uranium need to be understood to accurately predict the potential mobility and bioavailability of U(VI) in the subsurface that has been contaminated for many years. Many uranium contaminated sites such as the Hanford Site and the Rifle Site have existed for several decades. Therefore, U(VI) in those historically contaminated aged soils or sediments is likely to be associated with irreversible binding sites such as nanopore surfaces. Intragranular pore space often contains a significant fraction of the reactive surface area, and can thus strongly affect the transport of sorbing solutes although intragranular pore space within grain aggregates, grain fractures, and mineral surface coatings may contain a relatively small fraction of the total porosity within a porous medium (Hay et al., 2011). For example, in the Hanford 300A sediments, intragranular porosity is small, representing ~1% of the sediment skeletal volume, but the intragranular pore space contains a significant portion of the surface area (~20–35%), and thus provides a substantial portion of chemical sorption sites (Hay et al., 2011).

It is hypothesized that in the initial stage of contamination, contaminants fill macropores and sorb onto the surfaces of matrix aggregates, while with aging, contaminants enter into nanopores and micropores and trapped within these spaces, or penetrate into remote end of extremely narrow and tortuous paths, and hence become difficult for desorption (Steinberg et al., 1987; Pignatello and Xing, 1996; Eick et al., 1999). When the slow desorption of U(VI) from nanopores is ignored, the extent of desorption will be underestimated, and thus the mobility and bioavailability of U(VI) will be incorrectly predicted, resulting in the wrong choice of remediation technology (Pignatello and Xing, 1996). The reversible desorption model has failed to predict the long-term persistent release of contaminants to the environment and the existence of irreversible fractions has hindered the closure of many cleanup operations (Kan et al., 1998).

The slow desorption of U(VI) from sorption sites within nanoporous mineral surfaces is likely to cause the persistent contamination of groundwater U(VI) in a number of DOE sites (Zachara et al., 2016). Contaminant plumes in the aquifers of DOE sites can tail more extensively and require longer time to be flushed out, and consequently contaminated soils and sediments will exhibit greater resistance to biological, physical, or chemical remediation (Wu and Sun, 2010). On the other hand, contaminated soils and sediment containing higher amount of nanoporous mineral surfaces can be less hazardous than expected because U(VI) is less likely mobilized from nanoporous mineral surfaces. This study highlights that the irreversible sorption behavior of U(VI) and the effects of residence time on U(VI) desorption in contaminated soil or sediments that commonly contain nanoporous minerals need to be investigated through long-term sorption-desorption experiments prior to the implementation of remediation technologies.

Acknowledgement

This work is supported by the U.S. Department of Energy (DE-SC0002150). We are grateful to Dr. Hiromi Konishi for conducting HR-TEM and XRD analyses for the ORFRC soils.

References

Abbas, Z., Labbez, C., Nordholm, S., Ahlberg, E., 2008. Size-dependent surface charging of nanoparticles. J. Phys. Chem. C 112, 5715–5723.
Ahmed, I.A.M., Crout, N.M.J., Young, S.D., 2008. Kinetics of Cd sorption, desorption and fixation by calcite: a long-term radiotracer study. Geochem. Cosmochim. Acta 72, 1498–1512.
Ainsworth, C.C., Pilon, J.L., Gassman, P.L., Vandersluys, W.G., 1994. Cobalt, cadmium, and lead sorption to hydrous iron-oxide - residence time effect. Soil Sci. Soc. Am. J. 58, 1615–1623.
Anderson, R.T., Vrionis, H.A., Ortiz-Bernad, I., Resch, C.T., Long, P.E., Dayvault, R., Karp, K., Marutzky, S., Metzler, D.R., Peacock, A., White, D.C., Lowe, M., Lovley, D.R., 2003. Stimulating the in situ activity of Geobacter species to remove uranium from the groundwater of a uranium-contaminated aquifer. J. Appl. Environ. Microbiol. 69, 5884–5891.
Arai, Y., Sparks, D.L., 2002. Residence time effects on arsenate surface speciation at the aluminum oxide-water interface. Soil Sci. 167, 303–314.
Baborowski, M., Bozau, E., 2006. Impact of former mining activities on the uranium distribution in the River Saale (Germany). Appl. Geochem. 21, 1073–1082.
Backes, E.A., McLaren, R.G., Rate, A.W., Swift, R.S., 1995. Kinetics of cadmium and cobalt desorption from iron and manganese oxides. Soil Sci. Soc. Am. J. 59, 778–785.
Bai, J., Liu, C.X., Ball, W.P., 2009. Study of sorption-retarded U(VI) diffusion in Hanford silt/clay material. Environ. Sci. Technol. 43, 7706–7711.
Ball, W.P., Roberts, P.V., 1991. Long-term sorption of halogenated organic-chemicals by aquifer material. 1. equilibrium. Environ. Sci. Technol. 25, 1223–1237.
Banfield, J.F., Welch, S.A., Zhang, H.Z., Ebert, T.T., Penn, R.L., 2000. Aggregation-based crystal growth and microstructure development in natural iron oxyhydroxide biomineralization products. Science 289, 751–754.
Bargar, J.R., Reitmeyer, R., Davis, J.A., 1999. Spectroscopic confirmation of uranium(VI)-carbonato adsorption complexes on hematite. Environ. Sci. Technol. 33, 2481–2484.
Barnett, M.O., Jardine, P.M., Brooks, S.C., 2002. U(VI) adsorption to heterogeneous subsurface media: application of a surface complexation model. Environ. Sci. Technol. 36, 937–942.
Barnett, M.O., Jardine, P.M., Brooks, S.C., Selim, H.M., 2000. Adsorption and transport of uranium(VI) in subsurface media. Soil Sci. Soc. Am. J. 64, 908–917.
Barrett, E.P., Joyner, L.G., Halenda, P.P., 1951. The determination of pore volume and area distributions in porous substances. I. Computations from nitrogen isotherms. J. Am. Chem. Soc. 73, 373–380.
Bernhard, G., Geipel, G., Reich, T., Brendler, V., Amayri, S., Nitsche, H., 2001. Uranyl(VI) carbonate complex formation: validation of the Ca2UO2(CO3)(3)(aq.) species. Radiochim. Acta 89, 511–518.
Brina, R., Miller, A.G., 1992. Direct detection of trace levels of uranium by laser-induced kinetic phosphorimetry. Anal. Chem. 64, 1413–1418.
Bruemmer, G.W., Gerth, J., Tiller, K.G., 1988. Reaction-kinetics of the adsorption and desorption of nickel, zince and cadmium by goethite. 1. Adsorption and diffusin of metals. J. Soil Sci. 39, 37–52.
Campbell, K.M., Gallegos, T.J., Landa, E.R., 2015. Biogeochemical aspects of uranium mineralization, mining, milling, and remediation. Appl. Geochem. 57, 206–235.
Curtis, G.P., Davis, J.A., Naftz, D.L., 2006. Simulation of reactive transport of uranium(VI) in groundwater with variable chemical conditions. Water Resour. Res. 42.
Curtis, G.P., Fox, P., Kohler, M., Davis, J.A., 2004. Comparison of in situ uranium K-D values with a laboratory determined surface complexation model. Appl. Geochem. 19, 1643–1653.
Davis, J.A., Meece, D.E., Kohler, M., Curtis, G.P., 2004. Approaches to surface complexation modeling of uranium(VI) adsorption on aquifer sediments. Geochem. Cosmochim. Acta 68, 3621–3641.
Dong, W.M., Brooks, S.C., 2006. Determination of the formation constants of ternary complexes of uranyl and carbonate with alkaline earth metals (Mg2+, Ca2+, Sr2+, and Ba2+) using anion exchange method. Environ. Sci. Technol. 40, 4689–4695.

Dong, W.M., Tokunaga, T.K., Davis, J.A., Wan, J.M., 2012. Uranium(VI) adsorption and surface complexation modeling onto background sediments from the F-area Savannah River site. Environ. Sci. Technol. 46, 1565–1571.
Dong, W.M., Wan, J.M., 2014. Additive surface complexation modeling of uranium(VI) adsorption onto quartz-sand dominated sediments. Environ. Sci. Technol. 48, 6569–6577.
Eick, M.J., Naprstek, B.R., Brady, P.V., 2001. Kinetics of Ni(II) sorption and desorption on kaolinite: residence time effects. Soil Sci. 166, 11–17.
Eick, M.J., Peak, J.D., Brady, P.V., Pesek, J.D., 1999. Kinetics of lead adsorption/desorption on goethite: residence time effect. Soil Sci. 164, 28–39.
Ferreira, D.R., Schulthess, C.P., Giotto, M.V., 2012. An investigation of strong sodium retention mechanisms in nanopore environments using nuclear magnetic resonance spectroscopy. Environ. Sci. Technol. 46, 300–306.
Ford, R.G., Bertsch, P.M., Farley, K.J., 1997. Changes in transition and heavy metal partitioning during hydrous iron oxide aging. Environ. Sci. Technol. 31, 2028–2033.
Fox, P.M., Davis, J.A., Hay, M.B., Conrad, M.E., Campbell, K.M., Williams, K.H., Long, P.E., 2012. Rate-limited U(VI) desorption during a small-scale tracer test in a heterogeneous uranium-contaminated aquifer. Water Resour. Res. 48.
Fox, P.M., Davis, J.A., Zachara, J.M., 2006. The effect of calcium on aqueous uranium(VI) speciation and adsorption to ferrihydrite and quartz. Geochem. Cosmochim. Acta 70, 1379–1387.
Gadelle, F., Wan, J.M., Tokunaga, T.K., 2001. Removal of Uranium(VI) from contaminated sediments by surfactants. J. Environ. Qual. 30, 470–478.
Giammar, D.E., Hering, J.G., 2001. Time scales for sorption-desorption and surface precipitation of uranyl on goethite. Environ. Sci. Technol. 35, 3332–3337.
Gilbert, B., Ono, R.K., Ching, K.A., Kim, C.S., 2009. The effects of nanoparticle aggregation processes on aggregate structure and metal uptake. J. Colloid Interface Sci. 339, 285–295.
Guillaumont, R., Fanghanel, T., Neck, V., Fuger, J., Palmer, D.A., Grenthe, I., Rand, M.H., 2003. Update on the Chemical Thermodynamics of Uranium, Neptunium, Plutonium, Americium, and Technetium. Elsevier, Amsterdam.
Hatzinger, P.B., Alexander, M., 1995. Effect of aging of chemicals in soil on their biodegradability and extractability. Environ. Sci. Technol. 29, 537–545.
Hay, M.B., Stoliker, D.L., Davis, J.A., Zachara, J.M., 2011. Characterization of the intragranular water regime within subsurface sediments: pore volume, surface area, and mass transfer limitations. Water Resour. Res. 47.
Hochella, M.F., 2008. Nanogeoscience: from origins to cutting-edge applications. Elements 4, 373–379.
Hsi, C.K.D., Langmuir, D., 1985. Adsorption of uranyl onto ferric oxyhydroxides - application of the surface complexation site-binding model Geochim. Cosmochim. Acta 49, 1931–1941.
Jackson, M.L., Lim, C.H., Zelazny, L.W., 1986. Oxides, hydroxides, and aluminosilicates. In: Klute, A. (Ed.), Methods of Soil Analysis. Part 1, second ed. ASA and SSSA, Madison, WI.
Jeon, B.H., Kelly, S.D., Kemner, K.M., Barnett, M.O., Burgos, W.D., Dempsey, B.A., Roden, E.E., 2004. Microbial reduction of U(VI) at the solid-water interface. Environ. Sci. Technol. 38, 5649–5655.
Jung, H.B., Boyanov, M.I., Konishi, H., Sun, Y.B., Mishra, B., Kemner, K.M., Roden, E.E., Xu, H.F., 2012. Redox behavior of uranium at the nanoporous aluminum oxide-water interface: implications for uranium remediation. Environ. Sci. Technol. 46, 7301–7309.
Jung, H.B., Xu, H.F., Konishi, H., Roden, E.E., 2016. Role of nano-goethite in controlling U(VI) sorption-desorption in subsurface soil. J. Geochem. Explor. 169, 80–88.
Kan, A.T., Fu, G., Hunter, M., Chen, W., Ward, C.H., Tomson, M.B., 1998. Irreversible sorption of neutral hydrocarbons to sediments: experimental observations and model predictions. Environ. Sci. Technol. 32, 892–902.
Kelly, S.D., Kemner, K.M., Carley, J., Criddle, C., Jardine, P.M., Marsh, T.L., Phillips, D., Watson, D., Wu, W.-M., 2008. Speciation of uranium in sediments before and after in situ biostimulation. Environ. Sci. Technol. 42, 1558–1564.
Kohler, M., Curtis, G.P., Meece, D.E., Davis, J.A., 2004. Methods for estimating adsorbed uranium(VI) and distribution coefficients of contaminated sediments. Environ. Sci. Technol. 38, 240–247.
Kurttio, P., Auvinen, A., Salonen, L., Saha, H., Pekkanen, J., Makelainen, I., Vaisanen, S.B., Penttila, I.M., Komulainen, H., 2002. Renal effects of uranium in drinking water. Environ. Health Perspect. 110, 337–342.
Li, Z., Hofmann, A., Wolthers, M., Thomas, P., 2012. Reversibility of cadmium sorption to calcite revisited. J. Colloid Interface Sci. 368, 434–442.
Liu, C.X., Shi, Z.Q., Zachara, J.M., 2009. Kinetics of uranium(VI) desorption from contaminated sediments: effect of geochemical conditions and model evaluation. Environ. Sci. Technol. 43, 6560–6566.
Liu, C.X., Zachara, J.M., Qafoku, N.P., Wang, Z.M., 2008. Scale-dependent desorption of uranium from contaminated subsurface sediments. Water Resour. Res. 44.
Loganathan, V.A., Barnett, M.O., Clement, T.P., Kanel, S.R., 2009. Scaling of adsorption reactions: U(VI) experiments and modeling. Appl. Geochem. 24, 2051–2060.
Maher, K., Bargar, J.R., Brown, G.E., 2013. Environmental speciation of actinides. Inorg. Chem. 52, 3510–3532.
McBriarty, M.E., Soltis, J.A., Kerisit, S., Qafoku, O., Bowden, M.E., Bylaska, E.J., De Yoreo, J.J., Ilton, E.S., 2017. Trace uranium partitioning in a multiphase nano-FeOOH system. Environ. Sci. Technol. 51, 4970–4977.
McBride, M.B., 1994. Environmental Chemistry in Soils. Oxford University Press, Oxford.
McLaren, R.G., Backes, C.A., Rate, A.W., Swift, R.S., 1998. Cadmium and cobalt desorption kinetics from soil clays: effect of sorption period. Soil Sci. Soc. Am. J. 62, 332–337.
McLaren, R.G., Lawson, D.M., Swift, R.S., 1986. Sorption and desorption of cobalt by soils and soil components. J. Soil Sci. 37, 413–426.
Moon, J.W., Roh, Y., Phelps, T.J., Phillips, D.H., Watson, D.B., Kim, Y.J., Brooks, S.C., 2006. Physicochemical and mineralogical characterization of soil-saprolite cores from a field research site. Tennessee. J. Environ. Qual. 35, 1731–1741.
Parkhurst, D.L., Appelo, C.A.J., 1999. User's Guide to PHREEQC (Version 2)—a Computer Program for Speciation, Batch-Reaction, One-Dimensional Transport, and Inverse Geochemical Calculations, Water-Resources Investigations Report 99-4259. U.S. Geological Survey, Denver, Colorado.
Phillips, E.J.P., Landa, E.R., Lovley, D.R., 1995. Remediation of uranium contaminated soils with bicarbonate extraction and microbial U(VI) reduction. J. Ind. Microbiol. 14, 203–207.
Pignatello, J.J., Xing, B.S., 1996. Mechanisms of slow sorption of organic chemicals to natural particles. Environ. Sci. Technol. 30, 1–11.
Prelot, B., Lantenois, S., Chorro, C., Charbonnel, M.C., Zajac, J., Douillard, J.M., 2011. Effect of nanoscale pore space confinement on cadmium adsorption from aqueous solution onto ordered mesoporous silica: a combined adsorption and flow calorimetry study. J. Phys. Chem. C 115, 19686–19695.
Qafoku, N.P., Zachara, J.M., Liu, C.X., Gassman, P.L., Qafoku, O.S., Smith, S.C., 2005. Kinetic desorption and sorption of U(VI) during reactive transport in a contaminated Hanford sediment. Environ. Sci. Technol. 39, 3157–3165.
Senapati, S., Chandra, A., 2001. Dielectric constant of water confined in a nanocavity. J. Phys. Chem. B 105, 5106–5109.
Singer, D.M., Guo, H., Davis, J.A., 2014. U(VI) and Sr(II) batch sorption and diffusion kinetics into mesoporous silica (MCM-41). Chem. Geol. 390, 152–163.
Steinberg, S.M., Pignatello, J.J., Sawhney, B.L., 1987. Persistence of 1,2-dibromoethane in soils: entrapment in intraparticle micropores. Environ. Sci. Technol. 21, 1201–1208.
Stewart, B.D., Mayes, M.A., Fendorf, S., 2010. Impact of uranyl-calcium-carbonato complexes on uranium(VI) adsorption to synthetic and natural sediments. Environ. Sci. Technol. 44, 928–934.
Stoliker, D.L., Liu, C.X., Kent, D.B., Zachara, J.M., 2013. Characterizing particle-scale equilibrium adsorption and kinetics of uranium(VI) desorption from U-contaminated sediments. Water Resour. Res. 49, 1163–1177.
Stubbs, J.E., Veblen, L.A., Elbert, D.C., Zachara, J.M., Davis, J.A., Veblen, D.R., 2009. Newly recognized hosts for uranium in the Hanford Site vadose zone. Geochem. Cosmochim. Acta 73, 1563–1576.
Sylwester, E.R., Hudson, E.A., Allen, P.G., 2000. The structure of uranium (VI) sorption complexes on silica, alumina, and montmorillonite. Geochem. Cosmochim. Acta 64, 2431–2438.
Trivedi, P., Axe, L., 2000. Modeling Cd and Zn sorption to hydrous metal oxides. Environ. Sci. Technol. 34, 2215–2223.
van Beinum, W., Hofmann, A., Meeussen, J.C.L., Kretzschmar, R., 2005. Sorption kinetics of strontium in porous hydrous ferric oxide aggregates I. The Donnan diffusion model. J. Colloid Interface Sci. 283, 18–28.
van der Zee, C., Roberts, D.R., Rancourt, D.G., Slomp, C.P., 2003. Nanogoethite is the dominant reactive oxyhydroxide phase in lake and marine sediments. Geology 31, 993–996.
Waite, T.D., Davis, J.A., Payne, T.E., Waychunas, G.A., Xu, N., 1994. Uranium(VI) adsorption to ferrihydrite - application of a surface complexation model Geochim. Cosmochim. Acta 58, 5465–5478.
Wang, Y., 2014. Nanogeochemistry: nanostructures, emergent properties and their control on geochemical reactions and mass transfers. Chem. Geol. 378, 1–23.
Wang, Y., Gao, H., Xu, H.F., 2010. Nanogeochemistry: nanostructures and their reactivity in natural systems. In: Harmon, R.S., Parker, A. (Eds.), Frontiers in Geochemistry: Contribution of Geochemistry to the Study of the Earth. Blackwell Publishing Ltd, pp. 200–220.
Wang, Y.F., Bryan, C., Xu, H.F., Gao, H.Z., 2003. Nanogeochemistry: geochemical reactions and mass transfers in nanopores. Geology 31, 387–390.
Wazne, M., Korfiatis, G.P., Meng, X.G., 2003. Carbonate effects on hexavalent uranium adsorption by iron oxyhydroxide. Environ. Sci. Technol. 37, 3619–3624.
Wu, W.L., Sun, H.W., 2010. Sorption-desorption hysteresis of phenanthrene - effect of nanopores, solute concentration, and salinity. Chemosphere 81, 961–967.
Yabusaki, S.B., Fang, Y., Long, P.E., Resch, C.T., Peacock, A.D., Komlos, J., Jaffe, P.R., Morrison, S.J., Dayvault, R.D., White, D.C., Anderson, R.T., 2007. Uranium removal from groundwater via in situ biostimulation: field-scale modeling of transport and biological processes. J. Contam. Hydrol. 93, 216–235.
Zachara, J., Brantley, S., Chorover, J., Ewing, R., Kerisit, S., Liu, C., Perfect, E., Rother, G., Stack, A.G., 2016. Internal domains of natural porous media revealed: critical locations for transport, storage, and chemical reaction. Environ. Sci. Technol. 50, 2811–2829.